Ocean Engineering 242 (2021) 110096

Contents lists available at ScienceDirect

Ocean Engineering

journal homepage: www.elsevier.com/locate/oceaneng

A compositional Eulerian approach for modeling oil spills in the sea

Benjamin Ivorra [a,*,1], Susana Gomez [b,1], Jesus Carrera [c,1], Angel M. Ramos [a,1]

[a] Interdisciplinary Mathematics Institute & Department of Applied Mathematics and Mathematical Analysis, Complutense University of Madrid, Spain
[b] Instituto de Matemáticas Aplicadas y Sistemas, Universidad Nacional A. de México, Mexico
[c] Institute of Environmental Assessment and Water Research (IDAEA), CSIC, Spain

ARTICLE INFO

Dataset link: https://www.ucm.es/momat/software-momat

Keywords:
Oil spills in the sea
Compositional Eulerian model
Oil component behavior
Ageing of the oil
Coastal pollution risk analysis
Nonlinear diffusion

ABSTRACT

We present a Compositional Eulerian model to forecast the evolution of oil spills in the sea. The model allows studying the fate of not only the oil concentration but also of each component (e.g., volatile, non-volatile, water in the oil). Therefore, the problem is formulated as a conservation equation for each component, plus an equation to estimate the age of the oil, which allows us to assess weathering processes (e.g., evaporation, natural dispersion, emulsion) and the associated changes in oil properties. We describe an efficient implementation, using second order numerical schemes for advection and nonlinear diffusion terms, to reduce numerical diffusion. We perform numerical experiments, based on real and synthetic cases, to illustrate and validate the capabilities of our model to forecast the evolution of oil spills and to perform environmental risk analysis in the case of a potential accident.

1. Introduction

Oil spills in the ocean receive significant public attention and their remediation is costly. Forecasting by means of oil spill fate models is needed both to "get ahead of questions and concerns by the public" (Fingas, 2016) and to generate the information needed for the control and management of the spill (Comerma et al., 2006). Both needs imply that forecast has to be done as fast and accurately as possible. Models can also be used in preventive mode for environmental impact assessment and to plan emergency actions in response to hypothetical spills. In short, improvements to the ocean oil spills models become invaluable for addressing public concerns, designing remediation actions, and preparing contingency plans (see, e.g., Amir-Heidari and Raie (2019))

Oil spill modeling is complex because numerous processes are involved and because mathematical representation of each process is in itself complex. This complexity has led to specialists talking of "oil spill science" (Fingas, 2013). The spill fate is affected by transport processes, such as advection (i.e., dragging of the oil by wind, currents and wave fronts) or diffusion (i.e., spreading driven by waves and local fluctuations of wind and current or by gravity and thickness variations). Fate is also affected by weathering processes such as evaporation (i.e., transfer of oil to the atmosphere), dispersion (i.e., transfer of oil to the water column as oil droplets), dissolution (i.e., transfer of oil to the water column as solutes), emulsification (i.e., dispersion of water droplets into the oil, forming a new phase, "chapapote"), photo-oxidation (i.e., oxidation of oil by sun light), biodegradation (i.e., oxidation of oil by microorganisms), etc. (for detailed descriptions of these processes see e.g., Comerma et al. (2008), Reed et al. (2017) and Ward et al. (2018))

An additional difficulty is that most of the above processes depend on the composition of the oil. Oil consists of numerous components and the composition evolves in time, which affects the properties of the slick. For example, the boiling point and vapor pressure curve are different for each component. Evaporation is relevant for the light molecular weight components, but negligible for high molecular weight, so that it is frequent to distinguish between volatile and non-volatile components (e.g., Fingas (2016)). Emulsification concentrates on the non-volatile fraction because the "water-in-oil" suspension stability requires a minimum fraction of asphaltenes (high molecular weight, non-volatile) (e.g. Xie et al. (2007)). The latter implies that often, emulsification occurs only after significant evaporation has occurred (Xie et al., 2007). Dispersion is also sensitive to composition (e.g. Fingas (2014)). That is, the relevance of each weathering process may depend not only on the initial oil composition, but also on its time evolution. Most models simulate the oil slick as a single component (e.g., Spaulding (2017a))]) or using "pseudo-components"(as explained below) and represent weathering processes through empirical equations, instead

* Corresponding author.
E-mail addresses: ivorra@mat.ucm.es (B. Ivorra), susanag77@gmail.com (S. Gomez), jesus.carrera.ramirez@gmail.com (J. Carrera), angel@mat.ucm.es (A.M. Ramos).
[1] All authors contributed equally to the work.

https://doi.org/10.1016/j.oceaneng.2021.110096
Received 30 April 2021; Received in revised form 28 September 2021; Accepted 22 October 2021
Available online 9 November 2021

of simulating ageing explicitly. Still, these observations suggest that accurate forecasting would require modeling explicitly the composition of oil.

Accurate forecasting also demands accurate representation of transport processes. Most spill models and software adopt Lagrangian formulations (see, e.g., Sayol et al. (2014) or Spaulding (2017b)), which track the location of the oil through the distribution of oil particles in space (at the sea surface and in the water column) and time. Lagrangian formulations are convenient in that they model accurately advection and spreading mechanisms. However, they may need large memory and computation times, depending on number of particles needed to obtain sufficient spatial resolution (see De Dominicis et al. (2013), Rye (1995) and Spaulding (2017b)). Also, care must be taken on random walk process adopted to represent diffusion (Nordam et al., 2019), and in general non-local processes such as weathering or turbulent diffusion. That is turbulent diffusion, causing mixing of adjacent oil compositions, cannot be expressed solely in terms of local compositions. This is especially relevant for weathering which depends non-linearly on composition.

Eulerian models have also been developed, using either pure Eulerian (e.g., Ivorra et al. (2017), Juvinao Barrios (2016)) or Eulerian–Lagrangian (e.g., Acevedo et al. (2009), Comerma (2004) and Moghaddam et al. (2013)) methods. Eulerian models are less extended because they are assumed to suffer from numerical diffusion. However, we have recently developed a methodology to minimize numerical diffusion by including a non-linear diffusion term to avoid infinite diffusion velocities (Ivorra et al., 2017). This methodology, originally developed to simulate the pumping effect of a skimmer (Alavani et al., 2010), and to design an optimal trajectory for the skimmer ship (Gomez et al., 2011) was tested on synthetic examples based on real data from the Prestige (González et al., 2006) and from the Oleg Nayedov oil spills, (Gomez et al., 2018).

Tracking the oil composition is essential for properly representing the spill fate (Spaulding, 2017b). Oil composition has been typically represented in Lagrangian formulations using "pseudo-components" (i.e., aggregates of actual components sharing similar properties). Examples include OSCAR (Reed et al., 2017), ADIOS (Lehr et al., 2002) or the model proposed in French McCay et al. (2016). Oil composition may change in space and time as a result of turbulent diffusion, which causes mixing across the slick, but mixing is not reproduced by any of these compositional Lagrangian codes. Mixing would require modeling mass exchange between Lagrangian particles, which is feasible, but non-trivial. Paradoxically, compositional modeling has never been attempted using Eulerian Formulations, despite the fact that these formulations represent explicitly turbulent diffusion mixing.

The objective of this paper is to propose a (pseudo-) Compositional Eulerian Model. To this end, we build a system of Partial Differential Equations (PDEs) to represent (1) the mass balance for each (pseudo-) component, so as to facilitate modeling non-local processes and, specifically, mixing within the slick, and (2) the evolution of oil age, so as to facilitate modeling of weathering processes. This formulation has been implemented on a package called SOSMAR (Software for Oil Spill Movement And Removal).

2. Methods

We consider a 2D spatial domain (also called computational domain) $\Omega \subset \mathbb{R}^2$, representing the relevant ocean surface (i.e., large enough to ensure that the pollutant stays within the domain during the simulation time interval $(0,T)$). We denote by $\partial\Omega_o$ the boundary of Ω in the open sea and by $\partial\Omega_c$ the boundary at the coast.

We denote by $c(x,y,t)$ the pollutant product (i.e., the mixture which includes oil and, in case of emulsion, water) areal concentration, measured as the mass of pollutant product per surface area, at point $(x,y) \in \Omega$ and time $t \in (0,T)$. We assume that the evolution of c is governed by five main effects, namely:

- Transport of the pollutant product by advection and diffusion.
- Spill of oil due to a, possibly moving, source.
- Natural dispersion of oil in the water column.
- Evaporation of the volatile components.
- Emulsion of water in oil.

We note that c does not only include oil but also include water in oil which

We neglect other processes because they are assumed small, at least at the beginning (but see Socolofsky et al. (2019)). Proper representation of these processes requires acknowledging that oil consists of several components. We present the general form of governing equations in Section 2.1. Then, we explain in detail a specific implementation of the above processes in Section 2.2,

2.1. General Eulerian compositional model

We assume that the oil consists of $N \in \mathbb{N}$ components. At this stage, components may represent actual components or pseudo-components (Spaulding, 2017b). Following the standard in reactive transport literature (e.g., Saaltink et al. (1998b)), we denote by $u_i(x,y,t)$, for $i \in \{1,\dots,N\}$, the areal concentration of component i at position (x,y) and time t. Therefore, $c(x,y,t) = \sum_{i=1}^{N} u_i(x,y,t)$.

To ensure that the slick width remains finite, we model diffusion with the non-linear formulation of Ivorra et al. (2017), which ensures that diffusion tends to zero at the slick edges. To this end, we write the diffusion tensor as $\mathbf{D} = \frac{c^\kappa}{c_{\text{ref}}^\kappa}\mathbf{d}$, with $\mathbf{d} = \begin{pmatrix} d_1 & 0 \\ 0 & d_2 \end{pmatrix}$, $d_1, d_2 > 0$, being the diffusion coefficients in the principal directions, c_{ref} is a reference pollutant product concentration and $\kappa > 0$.

We point out that we use a Eulerian model with a nonlinear diffusion term, which generates a free boundary given by the edge of the oil slick, moving with finite velocity. This is an alternative to Lagrangian schemes, which allow particles to follow a "random flight" instead of a "random walk", ensuring that the particles always have a physically reasonable velocity (see, e.g., Lynch et al. (2014) in particular, Chapter 4, Sections 4.2 and 4.4 and Gillespie (1996a,b)). The Eulerian approach that we propose here reduces diffusivity to zero outside the slick, which does not allow to compensate unresolved model eddies, but it is convenient to reproduce mixing terms with the oil slick, which may be relevant for other processes (e.g., dispersion or weathering). It is important to note that Lagrangian methods, as typically applied in oil slick modeling, do not reproduce mixing processes, which would be feasible, but difficult to do with particles. In summary, we adopt this formulation for three reasons:

1. to reduce numerical dispersion on the slick edges,
2. to reproduce mixing effects within the slick and
3. to avoid non-zero concentration at any distance after any $t > 0$.

The fact that we model the oil composition implies that we need a conservation equation for each component. We assume that all components are subject to the same transport processes, but we find two possible ways to represent diffusion:

- In the first approach, each component diffuses independently, although with the same diffusion tensor, which is the standard approach for reactive transport models (e.g. Saaltink et al. (1998a)). Then, we get a system of PDEs, with $i \in \{1,\dots,N\}$, of the form:

$$\frac{\partial u_i}{\partial t} - \boldsymbol{\nabla}\cdot(\mathbf{D}\boldsymbol{\nabla}u_i - \mathbf{v}u_i) = \sum_{p=1}^{M_i} f_{i,p}, \tag{1}$$

where $\mathbf{v}$ is the advection velocity, the terms $f_{i,p}$ are the sink/source terms of ith component, associated to the different processes indexed by $p \in \mathbb{N}$ (e.g., $p = 1$ for the spilling source, and oil weathering: dispersion $p = 2$, evaporation $p = 3$, emulsion

$p = 4$, that produce an ageing effect in the oil). Adding them up, we obtain

$$\frac{\partial c}{\partial t} - \nabla \cdot (\mathbf{D}\nabla c - \mathbf{v}c) = \sum_{i=1}^{N}\sum_{p=1}^{M_i} f_{i,p}. \tag{2}$$

- In the second approach, each component follows the transport process of the whole phase (i.e., depending on c). In this case, the model is given, with $i \in \{1, \dots, N\}$, by

$$\frac{\partial u_i}{\partial t} - \nabla \cdot ((\frac{1}{c}\mathbf{D}\nabla c - \mathbf{v}))u_i = \sum_{p=1}^{M_i} f_{i,p} \tag{3}$$

or equivalently

$$\frac{\partial u_i}{\partial t} - \nabla \cdot ((\mathbf{D}\nabla \log(c) - \mathbf{v}))u_i = \sum_{p=1}^{M_i} f_{i,p}. \tag{4}$$

Adding up these equations, we obtain

$$\frac{\partial c}{\partial t} - \nabla \cdot (\mathbf{D}\nabla c - \mathbf{v}c) = \sum_{i=1}^{N}\sum_{p=1}^{M_i} f_{i,p}. \tag{5}$$

We note that adding the components Eqs. (1) or (3) we get the same general model (5), which has been already used in Ivorra et al. (2017). However, the evolution of the components may be different in each case. In the first case, there is a mixing effect, since each component is diffusing independently and in the second case diffusion causes spreading but not local mixing, so that all the components follow the transport process of the whole phase. The choice is non-trivial. Molecular diffusion produces mixing, which would require the first approach, whereas turbulent diffusion may produce mixing (e.g., effect of waves) or not (e.g., effect of wind fluctuations). In this paper we use the first approach, pending further research on the issue.

2.2. An example

We consider three components, actually pseudo-components, with areal concentration u_i, $i \in \{1, 2, 3\}$, defined as:

- u_1 (kg m^{-2}) is the areal concentration of the non-volatile components of the oil spill (asphaltenes, resins, etc.) and also the oil fraction of emulsion. It is affected by dispersion, but not by evaporation.
- u_2 (kg m^{-2}) is the areal concentration of the light components of the oil spill (volatiles). It is affected by the natural dispersion and the evaporation processes.
- u_3 (kg m^{-2}) is the areal concentration of water in oil. It is affected by the natural dispersion process.

The choice of these components is largely conditioned by the fact that we will simulate weathering with empirical equations that were originally derived for an integrated slick. Therefore, in addition to those components, we need to model the age of the oil at each point and time, in order to properly represent weathering processes. Thus, we introduce $a(x, y, t)$ (s), age of the oil at position (x, y) at time t. The evolution of a is assumed to be affected by the same diffusion and advection processes than the oil. Thus, it is modeled by a diffusion–advection–reaction partial differential equation similar to the equations for u_1, u_2 and u_3 (Varni and Carrera, 1998). Thus, we consider the following system of equations:

$$\begin{cases} \frac{\partial u_1}{\partial t} - \nabla \cdot (\mathbf{D}\nabla u_1 - \mathbf{v}u_1) = f_{1,1} - f_{1,2}\frac{u_1}{c}\chi_{c>0}, & \text{in } \Omega \times (0,T), \\ \frac{\partial u_2}{\partial t} - \nabla \cdot (\mathbf{D}\nabla u_2 - \mathbf{v}u_2) = f_{2,1} - \left(f_{2,2}\frac{u_2}{c} + f_{2,3}(u_2 + u_3)\right)\chi_{c>0}, & \text{in } \Omega \times (0,T), \\ \frac{\partial u_3}{\partial t} - \nabla \cdot (\mathbf{D}\nabla u_3 - \mathbf{v}u_3) = -f_{3,2}\frac{u_3}{c}\chi_{c>0} + f_{3,4}, & \text{in } \Omega \times (0,T), \\ \frac{\partial a}{\partial t} - \nabla \cdot (\mathbf{D}\nabla a - \mathbf{v}a) = \chi_{c>0}, & \text{in } \Omega \times (0,T), \end{cases} \tag{6}$$

where $\chi_{c>0} = 1$ if $c > 0$ and 0 elsewhere, and with the following initial and boundary conditions:

$$\begin{cases} L\frac{\partial u_i}{\partial t} - \left[-\mathbf{D}\nabla u_i + \mathbf{v}u_i\right] \cdot \mathbf{n} = 0, \text{for } i = 1,2,3, & \text{on } \partial\Omega \times (0,T), \\ L\frac{\partial a}{\partial t} - \left[-\mathbf{D}\nabla a + \mathbf{v}a\right] \cdot \mathbf{n} = 0, & \text{on } \partial\Omega \times (0,T), \\ u_1(0) = u_{1,0}, u_2(0) = u_{2,0}, u_3(0) = u_{3,0}, a(0) = a_0, & \text{in } \Omega. \end{cases} \tag{7}$$

Here, L is the characteristic length of the size of the domain Ω, (typically the diameter of Ω), $u_{1,0}, u_{2,0}, u_{3,0}$ and a_0 are the initial distributions at time 0 of u_1, u_2, u_3 and a, respectively. Note that the two first boundary conditions represent transparent and absorbent boundaries that preserve the shape of the concentration near the boundary by removing the oil that reaches the boundary (Ivorra et al., 2017). In particular, we use these equations to simulate the beaching process. The mass of the ith component of oil reaching the coast ($\partial\Omega_c$) is recorded through

$$B_i(x) = \int_{t\in[0,T]} \left[-D\nabla u_i(x,t) + \mathbf{v}u_i(x,t)\right] \cdot \mathbf{n} \ \mathrm{d}t, \tag{8}$$

where $x \in \partial\Omega_c$ and $B_i(x)$ (kg m^{-1}) represents the mass of the oil component i, per meter of coastline, that has reached point x up to time T. Therefore, the total mass of the oil component i reaching the coastline is

$$M_i = \int_{\partial\Omega_c} B_i(x)\mathrm{d}x. \tag{9}$$

The $f_{i,p}$ sink/source terms in Eqs. (6) are given by

- Moving source of spill: $f_{i,1}(x,t) = g_i(x,t)\chi_{\gamma(t)}(x)$, where $g_i(x,t)$ is the mass of the ith component of the oil spilled by the source per unit of surface area and unit time (kg m^{-2} s^{-1}), and $\gamma(t) \subset \Omega$ is the extent of the spill at time t ($\chi_{\gamma(t)}(x) = 1$, if $x \in \gamma(t)$, and 0 elsewhere). We usually take the spill to be a (moving) point, in which case $\gamma(t)$ is the spill location at time t, so that $\chi_{\gamma(t)}(x) = \delta(x - \gamma(t))$, $\delta()$ is Dirac's delta, and $g_i(t)$ is the mass rate of the ith component of the spill (kg s^{-1})
- Dispersion: $f_{1,2} = f_{2,2} = f_{3,2} = Q_d$ represents the transfer of oil into the water column by wave action or sea turbulence per unit of surface area and per unit time (kg m^{-2} s^{-1}) at point x at time t. It can be obtained by using the Audunson formula (see Auduson (1980))

$$Q_d(x,t) = \lambda_0(\frac{W(x,t)}{W_0})^2,$$

where λ_0 is the coefficient of natural dispersion, W (m s^{-1}) is the wind velocity at 10 meters above the sea level, W_0 (m s^{-1}) is the wind speed at which λ_0 was estimated. Some typical values are $\lambda_0 = 0.1$ (kg m^{-2} s^{-1}) and W_0=8.5 (m s^{-1}). Other options, such as the Delvigne formula (Delvigne and Sweeney, 1988) are available in the literature.

Remark 1. Here, we are using the classical formulas for the natural dispersion found in the literature. These formulas do not take into account the weathering process.

- Evaporation (only applies to the volatile component): Here, in order to obtain an estimation of $f_{2,3}(x,t)$, we consider $f_{2,3}(x,t) = \frac{\partial F_v}{\partial t}(x,t)$ where $F_v(x,t)$ is the evaporated fraction at point (x,t) at time t (s). Following Stiver and Mackay (1984), F_v is given by

$$F_v(x,t) = \frac{\mathcal{T}(x,t)}{B\mathcal{T}_g}\log[1 + B\frac{\mathcal{T}_g}{\mathcal{T}(x,t)}\frac{K_m a(x,t)}{\xi(x,t)}\exp(A - B\frac{\mathcal{T}_i}{\mathcal{T}(x,t)})], \tag{10}$$

where $\xi(x,t)$ (m) is the thickness of the oil spill, $\mathcal{T}(x,t)$ (K) is the temperature, $\mathcal{T}_i$ (K) and $\mathcal{T}_g$ (dimensionless) are the initial point and gradient of the boiling curve (i.e., the curve corresponding

to the percentage of volume distillate vs the boiling temperature, obtained from distillation data), A and B are empirical constants, K_m is the mass transfer coefficient (s m^{-2}). We note that, in the literature (see, e.g., Fingas (2013)), the factor $K_m a(x,t)/\xi(x,t)$ is usually termed evaporative exposure (i.e., the area of oil exposed to evaporation) and denoted as $\Theta(x,t)$.

We note that a more precise approach would be to estimate $f_{2,3}$ by relating explicitly the dynamic of the evaporation process to historic data (such as temperature or wind). However, such estimation was not available in the literature for the specific oils used in the numerical experiments presented in Section 3. Thus, we have considered the formulas proposed above. This point could be improved in future works.

Remark 2. In cases when data of $\mathcal{T}_i$ and $\mathcal{T}_g$ are missing, it is possible to use empirical formulas, such as the one by Fingas (2013), based on the information given by the Distillation curves of the oil. See for instance the formulas proposed in Section 3.

- Emulsion:

$$f_{3,4}(x,t) = \left(\frac{u_3(x,t)}{c(x,t)} \frac{\partial c}{\partial t}(x,t) + K_e (W(x,t)+1)^2 (c(x,t) - \frac{u_3(x,t)}{Y_f}) \right) \chi_{F_v(x,t)>\bar{F}} \chi_{c(x,t)>0},$$

where K_e is the emulsion constant that depends of the oil type (s m^{-2}), Y_f is the maximum content of water (in percentage), W the wind velocity at 10 meters above sea level and $\chi_{F_v(x,y,t)>\bar{F}}$=1, if $F_v(x,y,t) > \bar{F}$ and 0 elsewhere. $\bar{F}$ is the evaporation threshold at which the emulsion starts. This formula is based on the model proposed by Fingas and Fieldhouse (2003, 2004).

Finally, we are interested in estimating the evolution of the rheological properties of the spilled oil: viscosity, density, and consequently, the thickness of the slick. The change of viscosity and density can be produced by three effects: Temperature ($\mathcal{T}$), Evaporation (F_v) and Emulsion ($Y = u_3/c$, is the emulsified fraction). In particular,

- **for viscosity:** We denote by $\nu(x,t)$ the viscosity in centistokes (cSt) of the oil spill at point (x) at time t. Following Comerma (2004), the evolution of ν is given by

$$\nu(x,t) = \nu_0 \exp\left[\frac{B_1 Y(x,t)}{1 - B_2 Y(x,t)}\right] \exp\left[B_3(\mathcal{T}(x,t) - \mathcal{T}_0)\right] \exp\left[B_4 F_v(x,t)\right], \tag{11}$$

where B_1, B_2, B_3 and B_4 are constants that must be experimentally calibrated for each type of oil, $\mathcal{T}_0$ is the reference temperature (K), ν_0 is the viscosity of the oil at the source at $\mathcal{T}_0$.

- **For density:** We denote by $\rho(x,t)$ the density of the oil spill (kg m^{-3}) at point (x) at time t. Following Comerma (2004), Lehr (2001), the evolution of ρ is given by

$$\rho(x,t) = Y(x,t)\rho_w + (1 - Y(x,t))\rho_0 \exp\left[1 - B_5(\mathcal{T}(x,t) - \mathcal{T}_0)\right]\left[1 + B_6 F_v\right], \tag{12}$$

where B_5 and B_6 are constant experimentally calibrated for each type of oil, ρ_w is the density of the sea water, $\mathcal{T}_0$ is e reference temperature (K), ρ_0 is density of the oil at the source at $\mathcal{T}_0$.

- **For thickness:** We denote by $\xi(x,t)$ (m) the thickness of the oil spill at point x at t. It is given by:

$$\xi(x,t) = \frac{c(x,t)}{\rho(x,t)}.$$

Remark 3. We have used here a two-dimensional model, which allows to reduce the computational time needed to solve it numerically. Of course, we are aware that this choice has some drawbacks. For instance, it neglects the trailing slick that may be created by submerged droplets surfacing upwind of the slick (see, e.g., Elliott et al. (1986), Johansen (1982)). An intermediate solution is to consider a two-compartment model, where oil can exchange between surface and submerged and back again. We did not do it here, to focus on the main novelties of the paper. This possibility will need to be addressed in the future.

2.3. Numerical implementation

To perform the numerical experiments that will be presented in Section 3, we consider a Finite volume scheme with superbee flux limiter for the discretization of System (6)–(7). As this scheme is quite similar to the one detailed in Ivorra et al. (2017), here, we only report the differences with respect to this previous work.

We assume a spatial domain $\Omega = (x_{1,\min}, x_{1,\max}) \times (x_{2,\min}, x_{2,\max})$. Given two positive integers I and J, we divide Ω into IJ rectangular control volumes (also called cells) denoted by $\Omega_{i,j}$, for $i = 1,\dots,I$, $j = 1,\dots,J$, and defined by

$$\Omega_{i,j} = (x_{1,\min} + (i-1)\Delta x_1, x_{1,\min} + i\Delta x_1) \times (x_{2,\min} + (j-1)\Delta x_2, x_{2,\min} + j\Delta x_2),$$

with $\Delta x_1 = x_{1,\max} - x_{1,\min}/I$, $\Delta x_2 = x_{2,\max} - x_{2,\min}/J$.

For the time discretization of the considered equations, we use a fully explicit forward Euler scheme. The nth time step length, denoted by Δt^n, is obtained, to ensure that the Courant–Friedrichs–Lewy (CFL) condition is satisfied at all cells, with $C = 1$ as the CFL constant.

Let $\xi_{i,j}$ be the center of the cell $\Omega_{i,j}$. On each cell $\Omega_{i,j}$, we compute $U_{i,j}^{k,n+1}$, for $i = 1,\dots,I$, $j = 1,\dots,J$, $k = 1,\dots,4$ and at time step n, which approximates the value of u_k (if $k = 1,2,3$) or a (if $k = 4$) at point $\xi_{i,j}$ and at time $\sum_{l=1}^{n} \Delta t^l$. For $U_{i,j}^{k,0}$ given, we apply the following discretized scheme:

$$U_{i,j}^{k,n} = U_{i,j}^{k,n-1} - \mathcal{D}_k(i,j,n-1) - \mathcal{A}_k(i,j,n-1) - \mathcal{R}_k(i,j,n-1), \tag{13}$$

where $\mathcal{D}_k(i,j,n-1)$, $\mathcal{A}_k(i,j,n-1)$ and $\mathcal{R}_k(i,j,n-1)$ correspond to the discretization scheme of the diffusion term, the advective term and the reaction term in the kth line of (6), respectively.

Here, $\mathcal{D}_k$ and $\mathcal{A}_k$ are identical to the schemes reported in Ivorra et al. (2017). Additionally, schemes $\mathcal{R}_k, k = 1,\dots,4$, are given by

- $\mathcal{R}_1(i,j,n) = \left(g_1(\sum_{i=1}^{n} \Delta t^l)\chi_{i,j}^{s,n} - f_{1,2}(\xi_{i,j}, \sum_{l=1}^{n} \Delta t^l) \frac{U_{i,j}^{1,n}}{C_{i,j}^n} \chi_{C_{i,j}^n>0} \right) \Delta t^n,$

where $\Omega_{i_{s,n},j_{s,n}}$ is the cell containing $\gamma(\sum_{l=1}^{n} \Delta t^l)$, $C_{i,j}^n = \sum_{k=1}^{3} U_{i,j}^{k,n}$ $\chi_{i,j}^{s,n} = 0$ if $\{i,j\} \neq \{i_{s,n}, j_{s,n}\}$, $\chi_{i,j}^{s,n} = 1$ if $\{i,j\} = \{i_{s,n}, j_{s,n}\}$.

- $\mathcal{R}_2(i,j,n) = \left(g_2(\sum_{l=1}^{n} \Delta t^l)\chi_{i,j}^{s,n} - f_{2,2}(\xi_{i,j}, \sum_{l=1}^{n} \Delta t^l) \frac{U_{i,j}^{2,n}}{C_{i,j}^n} \chi_{C_{i,j}^n>0} - f_{2,3}(\xi_{i,j}, \sum_{l=1}^{n} \Delta t^l) U_{i,j}^{2,n} \right) \Delta t^n.$

- $\mathcal{R}_3(i,j,n) = \left(-f_{3,2}(\xi_{i,j}, \sum_{l=1}^{n} \Delta t^l) \frac{U_{i,j}^{3,n}}{C_{i,j}^n} \chi_{C_{i,j}^n>0} - f_{3,4}(\xi_{i,j}, \sum_{l=1}^{n} \Delta t^l) \right) \Delta t^n.$

- $\mathcal{R}_4(i,j,n) = \left(\chi_{C_{i,j}^n>0} \right) \Delta t^n.$

This scheme is completed by the discrete version of the boundary conditions (7) reported in Ivorra et al. (2017).

In practice, Ω is not a rectangle. However, we can easily adapt the previous scheme (13) to the general case. For this aim, we consider that if $\xi_{i,j}$ is not offshore, $\mathcal{D}_k(i,j,n) = \mathcal{A}_k(i,j,n) = \mathcal{R}_k(i,j,n) \equiv 0$, at any time step n. Moreover, the boundary conditions (7) are applied to the edges of cells that: (i) are situated at the border of the computational domain; or (ii) separate cells corresponding to off shore and cells corresponding land areas (i.e., edges in $\partial\Omega_c$).

Furthermore, to compute numerically the value of $B_i(x_c, y_c)$ given by (8), with $i = 1,2,3$ and $(x_c, y_c) \in \partial\Omega_c$, we consider the following scheme. Let ξ_{i_c,j_c} the center of the cell Ω_{i_c,j_c} containing (x_c, y_c). We note that, as said previously, due to the considered rectangular control volumes, the edges corresponding to the coast in Ω_{i_c,j_c} can be situated

at north, south, east or west sides of the cell. For simplicity, here, we only detail the case when the coast is situated at the west-side of this cell. The proposed scheme can be easily adapted when the coast is situated in one or several other directions. For this case, we compute

$$\hat{B}_i(i_c,j_c) = \sum_{k=1}^{n_f} \Delta t^k \left[\max\{0, o^{n_f-1}_{1,i_c,j_c-\frac{1}{2}}\} U^{n_f-1}_{i_c,j_c} + \min\{0, o^{n_f-1}_{1,i_c,j_c-\frac{1}{2}}\} U^{n_f-1}_{1,j} - \left(\frac{C^{n_f-1}_{i_c,j_c} + C^{n_f-1}_{i_c+1,j_c}}{2c_{\text{ref}}} \right)^{\kappa} \frac{d_1}{\Delta x_1} \left(U^{n_f-1}_{i_c+1,j_c} - U^{n_f-1}_{i_c,j_c} \right) \right], \tag{14}$$

where n_f is the final time step of the simulation, $v^n_{1,i,j-\frac{1}{2}} = v_1((x_{1,\min} + i\Delta x_1, x_{2,\min} + (j-\frac{1}{2})\Delta x_2), \sum_{i=1}^{n} \Delta t^i)$ and $\mathbf{v}(x,t) = (v_1(x,t), v_2(x,t))$ is the advection velocity field.

The value of M_i defined by (9), with $0 = 1, 2, 3$, is approximated by considering

$$M_i = \sum_{(i_c,j_c)\in\Gamma_c} \hat{B}_i(i_c,j_c) L_c,$$

where $\Gamma_c = \{(i_c,j_c)$, with $i_c = 1,\dots,I$ and $j_C = 1,\dots,J$ such that $\Omega_{i_c,j_c} \bigcap \partial\Omega_c \neq \emptyset\}$ and L_c is the length of the edges of Ω_{i_c,j_c} corresponding to the coast.

Finally, to compute the value of the viscosity ν and the density ρ, in a cell $\Omega_{i,j}$ at time step n, we evaluate the expressions (11) and (12) at the center of the cell $\xi_{i,j}$ at time step n.

3. Numerical experiments, results and discussion

In this section, we perform different numerical experiments to illustrate the capabilities of our model to forecast the evolution of a particular oil spill (see Section 3.1) and to perform environmental risk assessment in the case of a possible oil spill accident (Section 3.2).

All the experiments presented here are performed using our software SOSMAR (Software for Oil Spill Movement And Removal), which implements in Matlab the scheme presented in Section 2.3. More information about SOSMAR can be found at the following URL:

https://www.ucm.es/momat/sosmar

We have used a computer with an Intel I9-7920X with 2.90 GHz CPU, a Nvidia GTX 2060 GPU and 64 GB of Ram.

3.1. Validation considering the Prestige case

We focus here on the ability of our model to generate reliable forecasts. To do so, we perform numerical experiments based on meteorological and oil characteristics data from the Prestige oil spill hazard (2002, Spain) and compare the obtained forecast with available real observations and experimental studies (Section 3.1).

(a) Context:

On November 13th, 2002, the 'Prestige' ship started to leak oil in open sea near the Galician coasts, in Spain (Castanedo et al., 2006; Albaigés et al., 2010; Albaigés Riera et al., 2006). The Spanish Authorities decided some hours later, to send the ship far away from the Spanish coastline. On November 19th, 2002, the ship sank in the Atlantic Ocean. It is estimated that some 63,000 tons of crude oil were spilled during this incident, polluting thousands of kilometers of coast in Spain, France and Portugal (Balseiro et al., 2003).

Here, our objective is to use the numerical model proposed in Section 2.3, to simulate the oil concentration evolution from the beginning of the Prestige event, on November 13th, 2002 at 15:00, up to the November 17th, 2002 at 9:00. This final date was chosen because the only available clear satellite image of the whole situation was taken this day, before the Prestige ship broke up. After that, other satellite images are available, but with limited geographical area coverage.

(b) Data and Parameters:

To perform this numerical experiment, the simulation area was set to $\Omega \subset [-12.5, -8.5] \times [42, 44.2]$ (in longitude–latitude coordinate system), which is assumed to be large enough to ensure that the slick remains within this domain during the considered time interval. For the numerical finite volume scheme introduced above, we considered a 200 × 200 rectangular spatial mesh (i.e., each cell of size 1.2 km × 1.6 km) and a time step set to the minimum value between 15 min and the time step required by the CFL condition. The trajectory followed by the Prestige ship was taken from the literature (Castanedo et al., 2006; Montero et al., 2003). The simulation area (sea and coastal areas) and the trajectory of the Prestige ship are displayed in Fig. 1.

The advection velocity field $\mathbf{v} = (v_x, v_y)$ was built by considering:

- $\mathbf{v_w} = (v_{w,x}, v_{w,y})$: The velocity field of the wind at 10 meters from the surface.
- $\mathbf{v_s} = (v_{s,x}, v_{s,y})$: The sea surface current velocity field.
- $\mathbf{v_d} = (v_{d,x}, v_{d,y})$: The Stokes drift velocity field in the direction of wave propagation.

Those fields were estimated by considering historical discrete data (corresponding to our simulation dates) provided by the research center Mercator Ocean (see the Copernicus Marine Service URL: https://marine.copernicus.eu) and completed by using 2D spline interpolation to be able to obtain values at points with no data. Let $\mathbf{v_t} = \left[\frac{v_{s,x}+v_{d,x}}{|v_{s,x}+v_{d,x}|} \min\{|v_{s,x}+v_{d,x}|, \max\{|v_{s,x}|, |v_{d,x}|\}\}, \frac{v_{s,y}+v_{d,y}}{|v_{s,y}+v_{d,y}|} \min\{|v_{s,y}+v_{d,y}|, \max\{|v_{s,y}|, |v_{d,y}|\}\} \right]$ (a component would be 0 if the corresponding denominator in the previous formula is 0), we have considered (see, e.g., van den Bremer and Breivik (2018), Bird et al. (2006) and Macías et al. (2004))

$$\mathbf{v} = \mathbf{v_t} + w_d \left(\mathbf{v_w} - \mathbf{v_t} \right),$$

where w_d is the drag factor of the contribution of the wind to the advection term. Here, $w_d = 0.03$ (Ivorra et al., 2017).

The oil carried by the Prestige ship was heavy fuel oil number 6 (of Type M-100). According to laboratory experiments and estimations performed on some Prestige oil samples (see, e.g., Albaigés et al. (2010), Albaigés Riera et al. (2006)), this oil has the following characteristics:

- The American Petroleum Institute (API) gravity is 11.04 ° API.
- The density is $\rho_0 = 0.992$ kg l^{-1} at $\mathcal{T}_0 = 15$ °C.
- The viscosity is $\nu_0 = 100{,}000$ cSt at $\mathcal{T}_0 = 15$ °C.
- It contains some 5% of volatile components.
- Emulsification occurs (i.e., water in oil) and it is stable. Moreover, the maximum amount of water in emulsion is around 80%.

Furthermore, we completed those data by considering information relative to a similar product, namely the fuel oil number 5 (ESTS ♯ 586) (which is heavy fuel oil mixture composed by 20% of fuel oil number 2 and 80% of fuel oil number 6, and has an API gravity of 11.6° API), available at Fingas and Fieldhouse (2012), Wang et al. (2003):

- The evaporated fraction at position (x, y) and time t is given by
$$F_v(x,y,t) = \min\left\{ (-0.14 + 0.013\mathcal{T}(x,y,t))\sqrt{a(x,y,t)}, 0.05 \right\},$$
where $\mathcal{T}(x,y,t)$ is the temperature (°C). We note that we have limited the maximum value of this function to 5%, according to the estimated maximum evaporation fraction of fuel oil number 6.
- The maximum amount (in %) of water in emulsion is $Y_f = 0.78$. We note that this value is very close to the observation reported above (i.e., around 80%).

Finally, the remaining model parameters have been set to values found in the literature (Lehr, 2001; Mackay et al., 1980):

- The emulsion constant $K_e = 1.5 \times 10^{-6}$ (s m^{-2}).

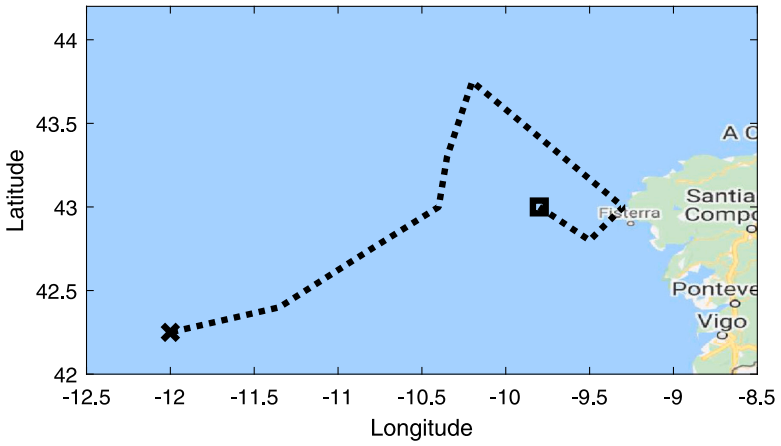

Fig. 1. Simulation domain and trajectory of the Prestige Ship used for the numerical experiments presented in Section 3.1. The square and cross represent the initial and final position of the ship, respectively. The map was generated with Google Maps.

- The evaporation threshold $\bar{F} = 0.05 \times 0.65 = 0.0325$ (%), as it is estimated that emulsion starts when 65% of the volatile components has evaporated.
- Regarding Eq. (11), we set $B_1 = 2.5, B_2 = 0.65, B_3 = 0.1$ and $B_4 = 75$.
- Regarding Eq. (12), we set $B_5 = 8 \times 10^{-4}$ and $B_6 = 0.2$.

To the best of our knowledge, the exact amount of oil leaked by the Prestige ship into the ocean from the 13th up to the 17th of November, remains unknown (Abascal et al., 2009; Castanedo et al., 2006; Montero et al., 2003). It is only known that around 54,000 tons of heavy/residual fuel oil were spilled into the sea before the Prestige ship broke on the 19th of November 2002. So, we assumed a continuous flow of 109.7 (kg s^{-1}), during the time interval of our simulation. Taking into account that 95% of this heavy fuel oil are non volatile components and 5% are volatile components, we set the spilling source as $g_1(t) = 104.2$ (kg s^{-1}) and $g_2(t) = 5.5$ (kg s^{-1}).

(c) Results and Discussion:

We used the software SOSMAR considering the above data and simulation parameters. The numerical simulation takes 160 CPU seconds.

In Fig. 2, we show the distributions of $c = u_1 + u_2 + u_3$, u_1 and u_3 returned by our model at the end of the simulation. The concentration u_2 is not reported as almost all of the volatile component has evaporated at the final date. In order to validate the geographical distribution forecast of our model, we present in Fig. 3 the satellite image taken by the Envisat ASAR satellite (property of the European Spatial Agency (ESA), and used here through the ESA Project 14161) of the oil spill situation on November 17th, 2002 at 9:00 and our distribution of c at the same date. We can observe that graphically both images present similarities regarding the general behavior of the oil spill shape. In particular, the areas of affected coastline are quite similar.

This indicates that the hydrodynamic data that we used in our simulation had a reasonable quality, allowing our model to predict, reasonably, the evolution of the oil concentration of the Prestige case. However, this figure also illustrates some limitations of our model, which is a simplification of the real situation. For example, our model fails to predict the splitting of the main oil leak in two branches.

In Fig. 4, we present several graphs corresponding to the evolution of the mass balance of the oil spill. More precisely:

- In Fig. 4-**(Top-Left)**, we draw the evolution of the amount (in barrels) of: (a) the total oil spilled, (b) the oil on the surface of the sea, (c) the oil reaching the coast, (d) the evaporated part of the oil, and (e) the oil affected by the natural dispersion process.
- In Fig. 4-**(Top Right)**, we report the evolution of the ratio (in percentage with respect to amount (a)) of the previous amounts (b) to (d) and the average ratio of emulsification of the oil on the surface (i.e., the percentage of water in oil).
- In Fig. 4-**(Bottom)**, we show the evolution of the amount (in kg) of concentrations c, u_1, u_2 and u_3 on the whole simulation domain.

As we can observe on Fig. 4-**(Top-Left)**, the first spots of oil could have reached the Spanish coastline during the first 18 h. This information is difficult to validate due to the lack of data about the first contaminated area in the coastline. Furthermore, according to Fig. 4-**(Top-Right)**, the emulsification process could have started after one and a half days, as the evaporation of the volatile components was quite fast. This estimation is within the range of times of weathering effects (see, e.g., Comerma (2004)). Indeed, it is commonly accepted that the evaporation process of a recently spilled oil occurs within the first days, whereas the emulsification process occurs between one day and one week. Furthermore, We observe that the ratio of evaporated product (5% of the total) and the emulsification (around 80%) are similar to the real observations (Albaigés et al., 2010; Albaigés Riera et al., 2006). Finally, in Fig. 4-**(Top-Bottom)**, we observe that when emulsification starts, the amount (in kg) of total product (i.e. "chapapote") dramatically increases. On the opposite, due to the low amount of volatile components in this particular oil and to the evaporation process, the concentration of component u_2 remains low.

The model also estimates the evolution of the density and the viscosity of the oil spilled on in the sea. At the end of the simulation, we observe that:

- The mean density of the oil is around 1.015 kg l^{-1} within a range between [0.990,1.020] (kg l^{-1}).
- The mean viscosity of oil is around 4,500,000 cSt and within a range between [75,000, 6,350,000] (cSt).

Those values are consistent with the fact that the density and the viscosity of the oil, may increase due to the weathering effects affecting the oil. In the literature (see, e.g., Fingas and Fieldhouse (2003)) it is reported that, for some heavy products, viscosity may increase more than 1000 times with respect to the initial value (in the results we present here, it increased up to 65 times).

From all those results, the evolution of the Prestige Oil spill obtained by our model is quite reasonable when compared to real observations. This indicates that our model can produce reliable forecasts for monitoring real oil spill events in the open sea.

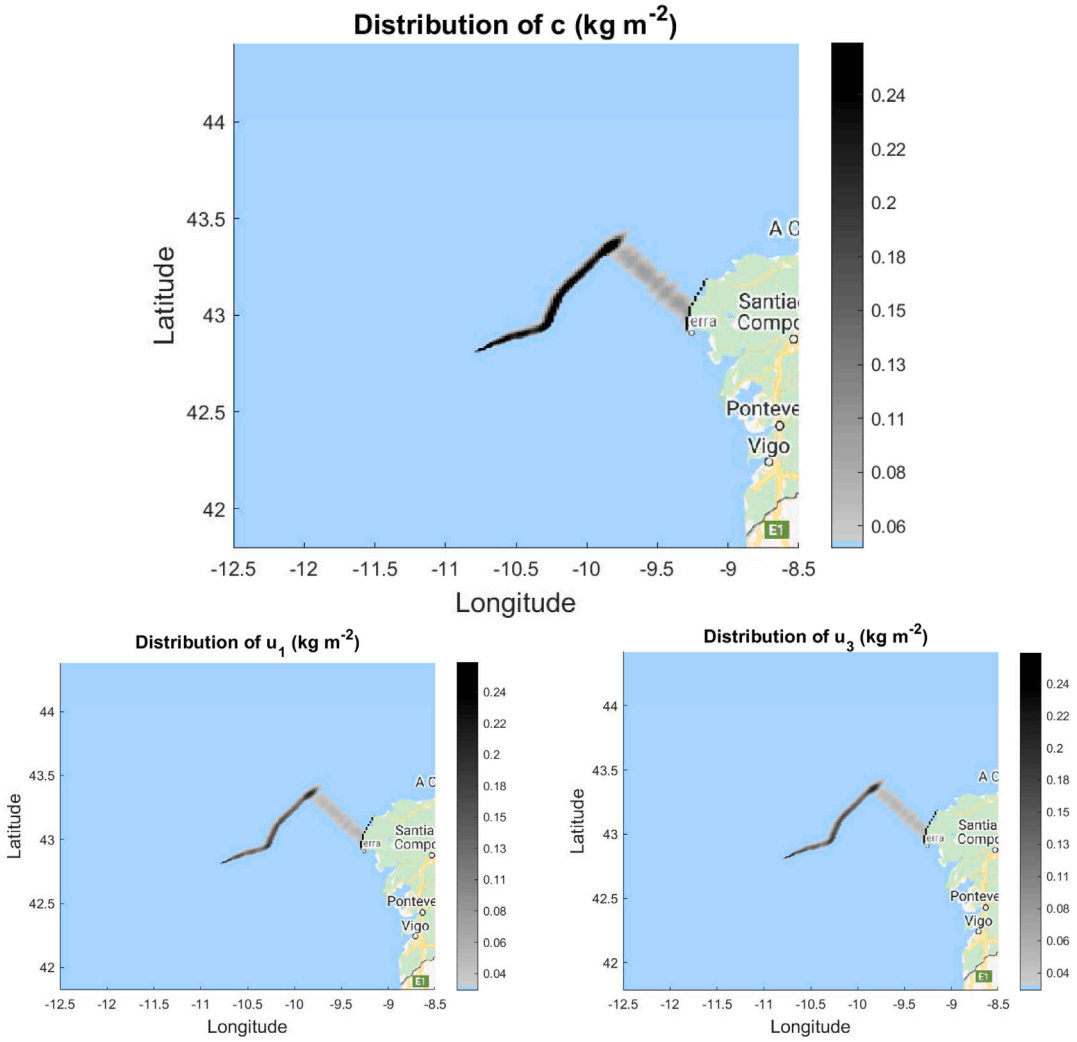

Fig. 2. Aerial concentration distribution (in kg m^{-2}) of c, u_1 and $u3$ obtained at the end of the experiment proposed in Section 3.1. The map was generated with Google Maps.

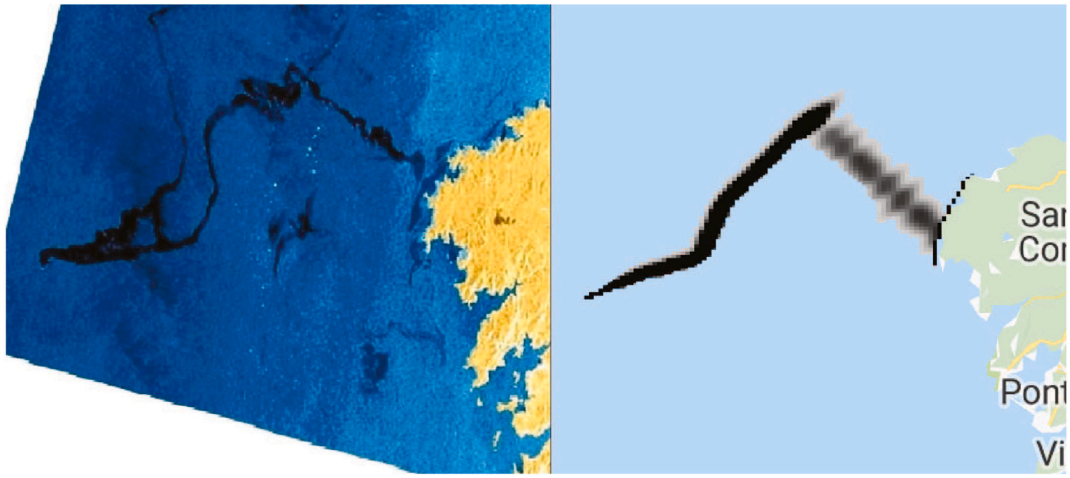

Fig. 3. **(Left)** Satellite image of the Prestige oil spill situation taken by the Envisat ASAR satellite (European Spatial Agency) on November 17th, 2002. **(Right)** Aerial concentration distribution (in kg m^{-2}) of c obtained at the end of the experiment proposed in Section 3.1. The colormap is the same as the one used in Fig. 2. The map was generated with Google Maps.

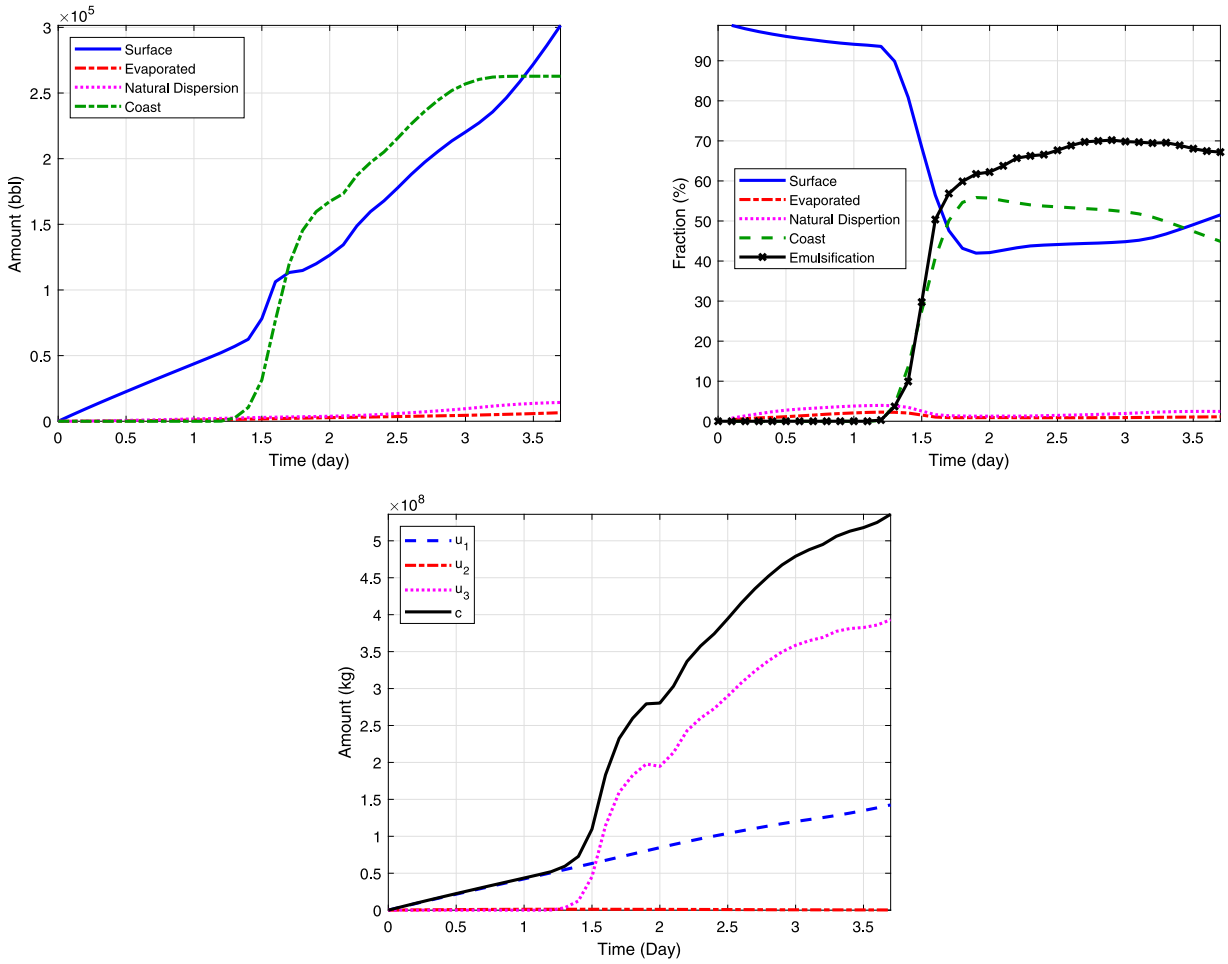

Fig. 4. Evolution of the mass balance of the oil spill, obtained at the end of the experiment proposed in Section 3.1. **(Top Left)** Amount (in barrels) of the total, surface, coastal, evaporated and dispersed oil. **(Top Right)** Ratio (in percentage with respect to the total amount of oil spilled) of the surface, coastal, evaporated and dispersed oil. The emulsification ratio (in percentage of water in oil) is also reported. **(Bottom)** Amount (in kg) of the concentrations c, u_1, u_2 and u_3 in the whole simulation domain.

3.2. Risk analysis

We show here the capability of our model to perform risk analysis, concerning the probable impact of the oil spill on the open sea and coastlines. First, in Section 3.2.1, to illustrate our approach, we consider a synthetic case based on meteorological data of the Mexican Gulf and data of an oil well present in the area. Finally, in Section 3.2.2, we validate our methodology by comparing a risk analysis performed at the beginning of the Grande-America Oil Spill (Biscay Gulf, 2018) with some real observations.

3.2.1. A synthetic Gulf of Mexico case

We consider a synthetic case for an oil extraction well situated between the coastline of Texas and Louisiana, USA, at coordinate −92.389,29 (in longitude–latitude coordinate system). At this coordinate the depth of the sea is around 23 m. The simulation area (sea and coastal areas) and the position of the oil extraction well are represented in Fig. 5.

We performed a risk analysis of a hypothetical oil spill due to an incident at this well, between the months of January and April. We run 100 scenarios, equidistant in time between January 1st and April 30th, 2019. For each scenario, we considered the data described below.

(a) Data and Parameters:

We consider a simulation area $\Omega \subset [-98,-89]\times[27,30]$ (in longitude–latitude coordinate system). We discretize this area with a 200 × 200 rectangular finite volumes mesh (i.e., each cell of size 2 km × 4 km) and a time step set to the minimum value between 1 h and the time step required by the CFL condition.

We assume that the oil is continuously spilled during 14 days.

As detailed in Section 3.1, the velocity fields of sea, wind and waves are provided by the research center Mercator Ocean (URL: http://www.mercator-ocean.fr).

The oil is assumed to be a light oil of the type 'South Louisiana' (ESTS ♯698). It has the following characteristics (Wang et al., 2005):

- The American Petroleum Institute (API) gravity is around 34.5 ° API.
- The density is $\rho_0 = 0.869$ kg l^{-1} at $T_0 = 15$ °C.
- The viscosity is $\nu_0 = 18.4$ cSt at $T_0 = 15$ °C.
- It is composed by around 31% of volatile components.
- For this type of oil, the emulsification is unstable. Thus, $Y_f = 0$.
- The evaporated fraction at position (x, y) and time t (min) is given by the following empirical formula

$$F_v(x,y,t) = \min\{(2.39 + 0.045\mathcal{T}(x,y,t))\ln a(x,y,t), 0.31\},$$

where $\mathcal{T}(x,y,t)$ is the temperature (°C).

Other coefficients are set to the values proposed in Section 3.1: $B_1 = 2.5$, $B_2 = 0.65$, $B_3 = 0.1$, $B_4 = 75$, $B_5 = 8\times10^{-4}$ and $B_6 = 0.2$.

We assume here, a continuous flow of 13.6 kg s^{-1}, during the time interval of our simulation. This corresponds to a total amount of 72,700 barrels (bbl) spilled in the sea during the spilling period. Taking into account that 69% of this oil are non-volatile components and 31% are

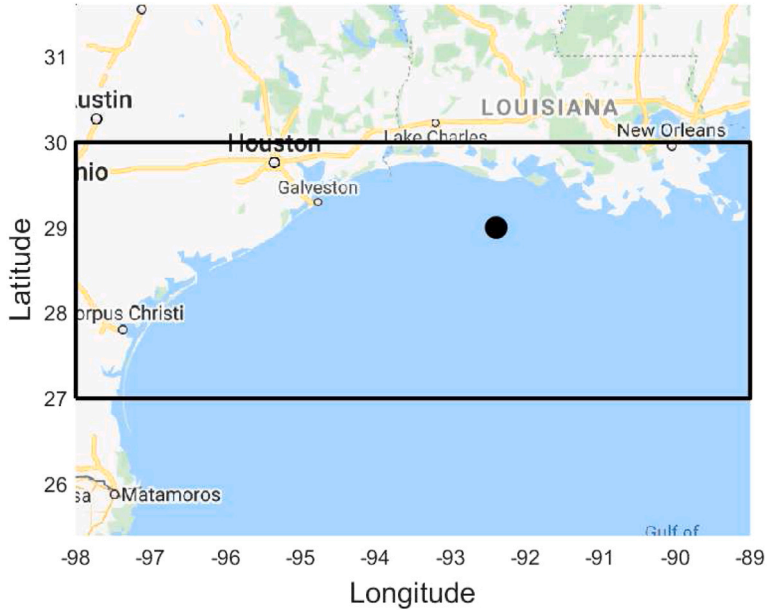

Fig. 5. Simulation domain (delimited by the black lines) used for the numerical experiments presented in Section 3.2.1. The circle represents the position of the oil offshore well. The map was generated with Google Maps.

volatile components, we set the spilling source as $f_{1,1}(t) = 9.4$ kg s^{-1} and $f_{2,1}(t) = 4.2$ kg s^{-1}.

(b) Results and Discussion:

The complete simulation takes around 6 h and 14 min.

Considering all scenarios, we report in Fig. 6 the probability of oil at the sea and the coast (computed as the percentage of scenarios for which a finite volume cell reaches an oil thickness of at least 10^{-7}m during the time interval, being this threshold the lower limit for oil visibility (Brown et al., 1996)). We also report, that the mean area of sea affected by the oil spill could reach 15,000 km^2. Considering the worst case (the maximum area), around 27,000 km^2 of the surface of the sea could be contaminated.

Next, we saw in Fig. 7, the mean mass balance evolution of the oil spill. The mean, minimum and maximum percentage of evaporated oil at the end of the simulation, could be 8%, 6% and 18%, respectively. The mean, minimum and maximum percentage of naturally dispersed oil at the end of the simulation, could reach 22%, 18% and 48%, respectively.

In 41% of the scenarios, the oil reached the coastline. For those cases, the mean time for reaching the coast is 198 h. The minimum time for reaching the coast is 100 h at the Rockefeller Wildlife Refuge. The mean amount of oil arriving to the coast during the simulation, is around 10,100 barrels (14% of the spilled oil), and the maximum amount of oil could reach 25,600 barrels (35% of the spilled oil). For those cases, the mean length of affected coastline could be 32 km, and 62 km for the worst case. This includes areas between Port Arthur (Texas) up to the Marsh Island (Louisiana). The evolution of the properties of the oil computed by our model shows that the viscosity and density of the oil reaching the coastline, are between 395 and 455 cSt and between 0.920 and 0.923 kg l^{-1}, respectively.

The results presented above, illustrate the relevance of such an analysis, to be able to estimate the risk of pollution due to an accident at an oil well and to design possible cleaning strategies (e.g., estimate the costs, schedule the cleaning time, etc.).

3.2.2. The Grande America case

In order to illustrate the efficiency of the risk analysis proposed in Section 3.2.1 on a real case, we briefly recall some results obtained during a risk analysis performed at the beginning (March 15th, 2019) of the Grande America oil spill, in the Biscay Bay (France and Spain), 2019. Then, we compare them to some real observations reported afterwards by authorities (Préfecture maritime de l'Atlantique, 2019).

This hazard started on March 10th, 2019 when a fire was declared in the ship Grande America. This ship transported around of 2,200 tons of intermediate fuel oil (IFO 380, ESTS ♯1955). Then, on March 12th, the ship sank in the Biscay Bay at position 46.04,−5.47 (in longitude–latitude coordinate system).

On March 15th, we studied this case with available data and published a risk analysis report of the sea and coastal pollution (see Ivorra et al. (2019)). More precisely, we considered the following data (Ivorra et al., 2019; Préfecture maritime de l'Atlantique, 2019; Yang et al., 2009):

- We run 90 scenarios equidistant in time between February 2nd and April 30th, 2018, assuming that the meteorological data would be similar to the present year.
- $\Omega \subset [-10, 0] \times [43, 51]$. We discretize this area with a 150 × 150 rectangular finite volumes mesh (i.e., each cell of size 5 km × 5 km).
- The American Petroleum Institute (API) gravity is around 14.7° API.
- The density is $\rho_0 = 0.967$ kg l^{-1} at $T_0 = 15$ °C.
- The viscosity is around $\nu_0 = 2{,}400$ cSt at $T_0 = 15$ °C.
- It is composed by 8% of volatile components.
- Emulsification is stable and the maximum amount (in %) of water in emulsion is $Y_f = 69$.
- The evaporated fraction at position (x, t) and time t (min) is given by

$$F_v(x, y, t) = \min\left\{(-0.12 + 0.013\mathcal{T}(x, y, t))\sqrt{a(x, y, t)}, 0.08\right\},$$

  where $\mathcal{T}(x, y, t)$ is the temperature (°C).
- $K_e = 1.5 \times 10^{-6}$ (s m^{-2}), $B_1 = 2.5, B_2 = 0.65, B_3 = 0.1$, $B_4 = 75$, $B_5 = 8 \times 10^{-4}$ and $B_6 = 0.2$.
- We assume a continuous oil leak during the 21 days of 11 kg s^{-1} and we set $f_{1,1}(t) = 10.1$ kg s^{-1} and $f_{2,1}(t) = 0.9$ kg s^{-1}.

Considering those data, the whole simulation took around 3 h. We present in Fig. 8 the simulation area, the probability of oil at the sea and the coast obtained by our software, and the front lines of the oil slick reported by French authorities the 21th and 25th of March

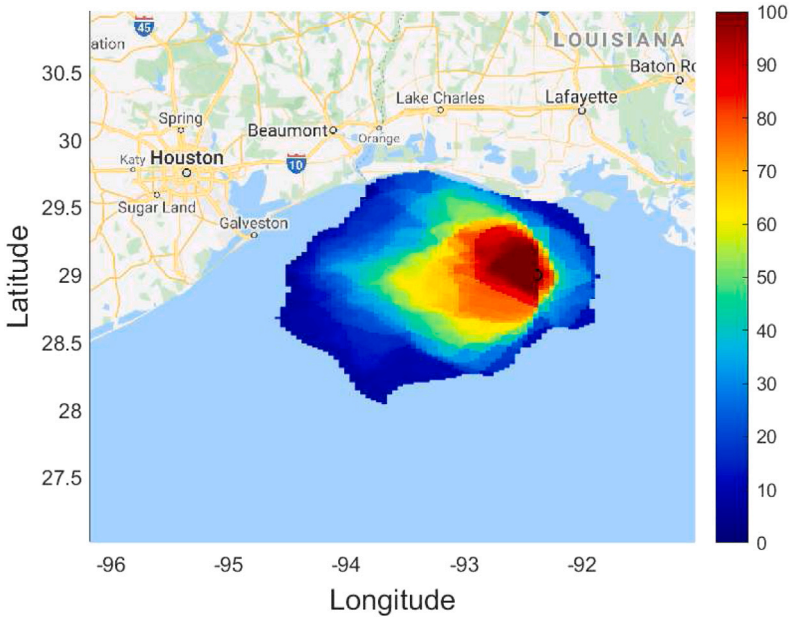

Fig. 6. Probability of oil in the sea and the coast obtained during the numerical experiments presented in Section 3.2.1. The circle represent the position of the oil offshore well. The map was generated with Google Maps.

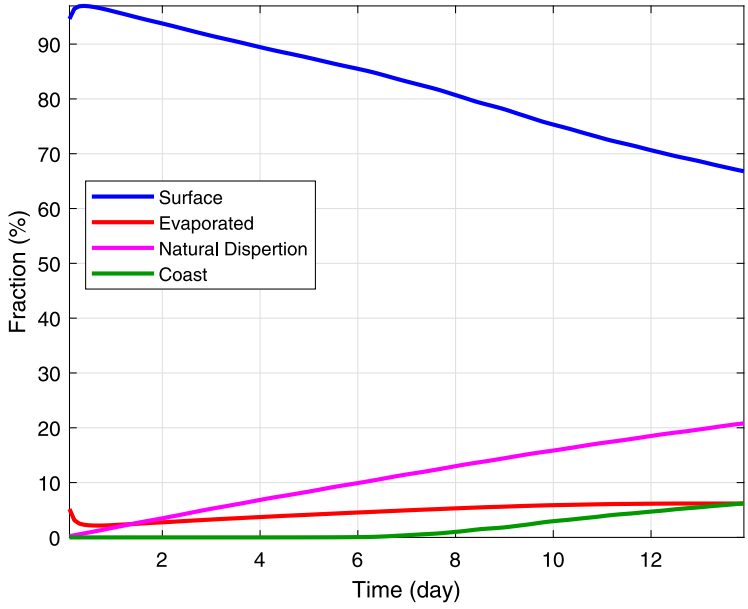

Fig. 7. Mean evolution of the mass balance of the oil spill, obtained at the end of the experiment proposed in Section 3.2.1: Ratio (in percentage with respect to the total amount of oil spilled) of the surface, coastal, evaporated and dispersed oil.

(see Préfecture maritime de l'Atlantique (2019), reports N° 14 and 18). We observe on this figure, that the front lines of the oil spill are included in an area with a probability of oil higher than 70%. We note that efficient cleaning methods were applied (not simulated in our study) and, thus, no oil spots reached the coastline. Taking into consideration that the period of simulation was quite long (3 weeks) and some data were unknown (i.e., the total amount spilled), these results show that our risk analysis methodology provides good results.

4. Conclusions

We have presented a new Compositional Eulerian formulation to simulate the transport and fate of an oil spill in the sea. The most singular features of this formulation is that it simulates the fate of different components of the oil. Assessing the time and space evolution of the slick components may be interesting not only for accurate representation of weathering processes, but also for monitoring and for remediation plans. The resulting PDE system includes an equation that describes the age of the slick in a continuous way. Ideally, age would not be explicitly required if composition was accurately known and the weathering processes could be described for each component. Since this knowledge is not yet available, we have used empirical equations for weathering processes that depend on age. It may be rightly argued that these equations were originally developed for Lagrangian formulations that do not reproduce turbulent mixing. Therefore, their direct use for Eulerian formulations, which model mixing explicitly, is not granted. Model results related to the weathering processes (such as, the evolution of oil viscosity and density, emulsification, and evaporation)

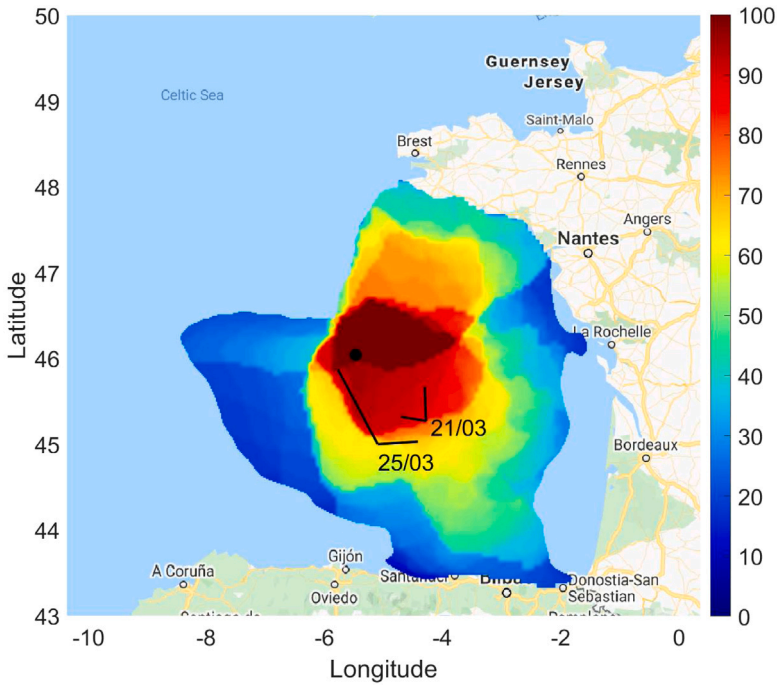

Fig. 8. Probability of oil in the sea and the coast obtained during the numerical experiments presented in Section 3.2.1. The circle represent the position of the ship Grande America. The continuous lines represent the front lines of the oil slick reported by French authorizes on the 21th and 25th of March, 2019. The map was generated with Google Maps.

reported in Section 3.1 were consistent with data reported in the literature. This suggest that their use for these cases is, at least approximately, appropriate. Still, further validation may be appropriate, especially in view of the tendency to model complex compositions, where explicit representation of mixing may be required.

We use advanced numerical methods to overcome traditional limitations of Eulerian formulations for oil spill simulation. Specifically, we adopt a non-linear diffusion term and a second order advective numerical scheme to minimize numerical diffusion. We introduce absorbent and transparent boundary conditions to preserve the shape of the spill near the boundaries, and to facilitate the computation and improve the accuracy of the simulation of the beaching process. The numerical solution, for three pseudo-components, has been implemented in software SOSMAR.(Software for Oil Spill Movement And Removal).

The formulation has been validated in two real oil spills cases. We have compared model results to satellite images and published information on the situation and characteristics of the oil after a period of time. Obtained results display similarities with real observations. The computation time is fair, which allows the use of refined grids to get the desired accuracy. Applicability of the formulation for risk analysis has been illustrated by application to (1) a synthetic example of a theoretical oil spill event in the north of the Gulf of Mexico, (2) a real case, where we can compare the obtained results with observations. This analysis could serve to quantify the costs of cleaning and to plan emergency spills response options.

Declaration of competing interest

The authors declare that they have no known competing financial interests or personal relationships that could have appeared to influence the work reported in this paper.

Software and/or data availability

All the experiments presented here are performed using our software SOSMAR (Software for Oil Spill Movement And Removal), which implements in Matlab the scheme presented in Section 2.3. More information about SOSMAR can be found at the following URL:

https://www.ucm.es/momat/sosmar

Some input data are detailed in this paper and the meteorological data, can be downloaded from the Copernicus Marine Service web-page:

https://marine.copernicus.eu

Data availability statement

The data that support the findings of this study are available from the corresponding author upon reasonable request. For information about SOSMAR, see https://www.ucm.es/momat/software-momat.

Acknowledgments

This work was carried out thanks to the financial support from the Spanish "Ministry of Science and Innovation" under Project PID2019-106337GB-I00 and the National University of Mexico Project PASPA, DGAPA. We also thank Nelson del Castillo, for his support in the elaboration of this article. Comments by two anonymous reviewers have contributed to improving the final version of the paper. Some of the figures proposed in this work include maps from the Google Map website (see, for instance, https://www.google.com/maps).

References

Abascal, A., Castanedo, S., Mendez, F., Medina, R., Losada, I., 2009. Calibration of a Lagrangian transport model using drifting buoys deployed during the prestige oil spill. J. Coast. Res. 251, 80–90.

Acevedo, A., Oliveira, A., Fortunato, A., Bertin, X., 2009. Aplication of an Eulerian-Lagragian oil spill modelling system to the Prestige accident: trajectory analysis. In: Journal of Coastal Research, 10th International Coastal Symposium, pp. 777–781.

Alavani, C., Glowinski, R., Gomez, S., Ivorra, B., Joshi, P., Ramos, A., 2010. Modelling and simulation of a polluted water pumping process. Math. Comput. Modelling 51 (5–6), 461–472.

Albaigés, J., Bernabeu, A., Castanedo, S., Jiménez, N., Morales-Caselles, C., Puente, A., Viñas, L., 2010. The prestige oil spill. In: Fingas, M. (Ed.), Oil Spill Science and Technology. Elsevier Science, pp. 515–545.

Albaigés Riera, J., Morales-Nin, B., Vilas, F., 2006. The prestige oil spill: A scientific response. Mar. Pollut. Bull. 53 (5), i.

Amir-Heidari, P., Raie, M., 2019. A new stochastic oil spill risk assessment model for Persian gulf: Development, application and evaluation. Mar. Pollut. Bull. 145, 357–369.

Auduson, T., 1980. The fate and weathering of surface oil from the Bravo Blowout. Mar. Environ. Res. 3, 35–61.

Balseiro, C., Carracedo, P., Gómez, B., Leitão, P., Montero, P., Naranjo, L., Penabad, E., Pérez-Muñuzuri, V., 2003. Tracking the Prestige oil spill: An operational experience in simulation at MeteoGalicia. Weather 58 (12), 452–458.

Bird, R., Stewart, W., Lightfoot, E., 2006. Transport Phenomena. In: Wiley International edition, Wiley.

Brown, H., Bittner, J., Goodman, R., 1996. The limits of visibility of spilled oil sheens. In: of Michigan, E.R.I. (Ed.), Proceedings of the Second International Airborne Remote Sensing Conference and Exhibition. In: ERIM Conferences, Michigan, vol. III, pp. 327–333.

Castanedo, S., Medina, R., Losada, I., Vidal, C., Méndez, F., Osorio, A., Juanes, J., Puente, A., 2006. The prestige oil spill in Cantabria (Bay of Biscay). Part I: Operational forecasting system for quick response, risk assessment, and protection of natural resources. J. Coast. Res. 1474–1489.

Comerma, E., 2004. Modelado numérico de la deriva y envejecimiento de los hidrocarburos vertidos al mar: aplicación operacional en la lucha contra las mareas negras (Ph.D. thesis). Universitat Politècnica de Catalunya, Spain.

Comerma, E., Espino, M., Daniel, P., Doré, A., Cabioch, F., 2008. An update of an oil spill model and its application in the Bay of Biscay: the weathering process. In: Oil and Hydrocarbon Spills III: Modelling, Analysis and Control. WIT Press, pp. 13–22.

Comerma, E., Espino, M., Salazar, M., Jerez, F., Madrigal, R., Arcilla, A., 2006. CAMCAT: an oil spill forecasting system for the Catalan-Balearic Sea based on the MFS products. Ocean Sci. Discuss. 3, 1791–1823.

De Dominicis, M., Pinardi, N., Zodiatis, G., Archetti, R., 2013. MEDSLIK-II, a Lagrangian marine surface oil spill model for short-term forecasting – Part 2: Numerical simulations and validations. Geosci. Model Dev. 6, 1871–1888.

Delvigne, G., Sweeney, C., 1988. Natural dispersion oil. Oil Chem. Pollut. 4, 281–310.

Elliott, A., Hurford, N., Penn, C., 1986. Shear diffusion and the spreading of oil slicks. Mar. Pollut. Bull. 17 (7), 308–313.

Fingas, M., 2013. Modeling oil and petroleum evaporation. J. Petroleum Sci. Res. 2 (3), 104–115.

Fingas, M., 2014. A review of natural dispersion models. In: International Oil Spill Conference Proceedings. pp. 1–18.

Fingas, M., 2016. Oil Spill Science and Technology, second ed. Gulf Professional Publishing.

Fingas, M., Fieldhouse, B., 2003. Studies of the formation process of water-in-oil emulsions. Mar. Pollut. Bull. 47 (9), 369–396.

Fingas, M., Fieldhouse, B., 2004. Formation of water-in-oil emulsions and application to oil spill modelling. J. Hard Mater. 107, 37–50.

Fingas, M., Fieldhouse, B., 2012. Studies on water-in-oil products from crude oils and petroleum products. Mar. Pollut. Bull. 64 (2), 272–283.

French McCay, D., Horn, M., Li, Z., Crowley, D., Spaulding, M., Mendelsohn, D., Jayko, K., Kim, Y., Isaji, J., Shmookler, R., Rowe, J., 2016. Simulation modeling of ocean circulation and oil spills in the gulf of Mexico. Appendix VI Data Collection, Analysis and Model Validation. Prepared By RPS ASA for the US Department of the Interior, Bureau of Ocean Energy Management, Gulf of Mexico OCS Region, New Orleans, la.

Gillespie, D., 1996a. Exact numerical simulation of the ornstein-uhlenbeck process and its integral. Phys. Rev. E 54, 2084–2091.

Gillespie, D., 1996b. The mathematics of Brownian motion and Johnson noise. Amer. J. Phys. 64 (3), 225–240.

Gomez, S., Ivorra, B., Ramos, A., 2011. Optimization of a pumping ship trajectory to clean oil contamination in the open sea. Math. Comput. Model. 54 (1–2), 477–489.

Gomez, S., Ivorra, B., Ramos, A., 2018. Designing optimal trajectories for a skimmer ship to clean, recover and prevent the oil spilled on the sea from reaching the coast. Appl. Math. Nonlinear Sci. 3 (2), 553–570.

González, M., Uriarte, A., Pozo, R., Collins, M., 2006. The prestige crisis: Operational oceanography applied to oil recovery, by the Basque fishing fleet. Mar. Pollut. Bull. 53 (5), 369–374, The Prestige Oil Spill: A Scientific Response.

Ivorra, B., Gomez, S., Glowinski, R., Ramos, A., 2017. Nonlinear advection—Diffusion—Reaction phenomena involved in the evolution and pumping of oil in open sea: Modeling, numerical simulation and validation considering the prestige and oleg naydenov oil spill cases. J. Sci. Comput. 70 (3), 1078–1104.

Ivorra, B., Gómez, S., Ramos, A., 2019. Current situation, Forecast and Risk Analysis for the Grande America Oil Spill started on March 12, 2019 in the Bay of Biscay. Technical Report, ResearchGate.

Johansen, O., 1982. Drift of Submerged Oil at Sea. Institutt for kontinentalsokkelundersøkelser rapporter;p 319/1.

Juvinao Barrios, D., 2016. Numerical Simulation of Oil Spills: Application to Coastal Zone (Master thesis E.T.S.I. de Minas Y Energia).

Lehr, W., 2001. Review of modeling procedures for oil spill weathering behavior. In: Brebbia, C. (Ed.), Oil Spill Modelling and Processes. WIT Press, pp. 51–90.

Lehr, W., Jones, R., Evans, M., Simecek-Beatty, D., Overstreet, R., 2002. Revisions of the ADIOS oil spill model. Environ. Model. Softw. 17 (2), 191–199.

Lynch, D., Greenberg, D., Bilgili, A., McGillicuddy, Jr., D., Manning, J., Aretxabaleta, A., 2014. Particles in the Coastal Ocean: Theory and Applications. Cambridge University Press.

Macías, J., Parés, C., Castro, M., 2004. Numerical simulation in oceanography. applications to the Alboran Sea and the Strait of Gibraltar. In: Ocean Circulation and Pollution Control — A Mathematical and Numerical Investigation: A Diderot Mathematical Forum. Springer Berlin Heidelberg, Berlin, Heidelberg, pp. 75–98.

Mackay, D., Trudel, K., Paterson, S., Research, C.E.E.B., Division, D., Directorate, C.E.I.C., 1980. A Mathematical Model of Oil Spill Behaviour. Research and Development Division, Environmental Emergency Branch.

Moghaddam, A., Attari, A., Dabir, B., 2013. A 2-D hybrid particle tracking/Eulerian-lagrangian model for oil spill problems. Indian J. Geo-Mar. Sci. 42 (1), 42–49.

Montero, P., Leitao, P., Penabad, E., Balseiro, C., Carracedo, P., Braunschweig, F., Fernandes, R., Gomez, B., Perez-Munuzuri, V., Neves, R., 2003. Modelling the oil spill track from Prestige-Nassau accident. In: EGS - AGU - EUG Joint Assembly. p. 12647.

Nordam, T., Nepstad, R., Litzler, E., Röhrs, J., 2019. On the use of random walk schemes in oil spill modelling. Mar. Pollut. Bull. 146, 631–638.

Préfecture maritime de l'Atlantique, 2019. Naufrage du navire Grande America dans le Golfe de Gascogne. Communiqué de presse, pp. 1–23.

Reed, M., Daling, P., Brakstad, O., Singsaas, I., Faksness, L., Hetland, B., Ekrol, N., 2017. Oscar: a multi-component 3-dimensional oil spill contingency and response model. In: Proceedings of the Arctic and Marine Oil Spill Program (AMOP) Technical Seminar, Vancouver, CA, vol. 31. pp. 663–680.

Rye, H., 1995. A multicomponent oil spill model for dissolved aromatic concentrations. Int. Oil Spill Conf. Proc. 1995 (1), 49–53.

Saaltink, M., Ayora, C., Carrera, J., 1998a. A mathematical formulation for reactive transport that eliminates mineral concentrations. Water Resour. Res. 34 (7), 1649–1656.

Saaltink, M.W., Ayora, C., Carrera, J., 1998b. A mathematical formulation for reactive transport that eliminates mineral concentrations. Water Resour. Res. 34 (7), 1649–1656.

Sayol, J., Orfila, A., Simarro, G., Conti, D., Renault, L., Molcard, A., 2014. A Lagrangian model for tracking surface spills and SaR operations in the ocean. Environ. Model. Softw. 52, 74–82.

Socolofsky, S., Gros, J., North, E., Boufadel, M., Parkerton, T., Adams, E., 2019. The treatment of biodegradation in models of sub-surface oil spills: A review and sensitivity study. Mar. Pollut. Bull. 143, 204–219.

Spaulding, M., 2017a. State of the art review and future directions in oil spill modeling. Mar. Pollut. Bull. 115 (1), 7–19.

Spaulding, M., 2017b. State of the art review and future directions in oil spill modeling. Mar. Pollut. Bull. 115 (1–2), 7–19.

Stiver, W., Mackay, D., 1984. Evaporation rate of spills of hydrocarbons and petroleum mixtures. Environ. Sci. Technol. 18, 834–840.

van den Bremer, T., Breivik, O., 2018. Stokes drift. Phil. Trans. R. Soc. A 376 (2111), 20170104.

Varni, M., Carrera, J., 1998. Simulation of groundwater age distributions. Water Resour. Res. 34 (12), 3271–3281.

Wang, Z., Hollebone, M., Fieldhouse, B., Sigouin, L., Landriault, M., Smith, P., Noonan, J., Thouin, G., 2003. Characteristics of Spilled Oils, Fuels, and Petroleum Products: 1. Composition and Properties of Selected Oils. Epa/600/r-03/072, National Exposure Research Laboratory Office of Research and Development United States Environmental Protection Agency.

Wang, Z., Yang, C., Fingas, M., Hollebone, B., Peng, X., Hansen, A., Christensen, J., 2005. Characterization, weathering, and application of sesquiterpanes to source identification of spilled lighter petroleum products. Environ. Sci. Technol. 39 (22), 8700—8707.

Ward, C., Sharpless, C., Valentine, D., French-McCay, D., Aeppli, C., White, H., Reddy, C., 2018. Partial photochemical oxidation was a dominant fate of Deepwater Horizon surface oil. Environ. Sci. Technol. 52 (4), 1797–1805.

Xie, H., Yapa, P., Nakata, K., 2007. Modeling emulsification after an oil spill in the sea. J. Mar. Syst. 68 (3–4), 489–506.

Yang, C., Wang, Z., Hollebone, B., Brown, C., Landriault, M., 2009. Characteristics of bicyclic sesquiterpanes in crude oils and petroleum products. J. Chromatogr. A 1216 (20), 4475–4484.